

High-Temperature Electrochemical Heat Pump Using a Water Gas Shift Reaction. Electrochemical Reduction of CO₂ to CO

Akimitsu Ishihara, Tomotaka Fujimori, Naobumi Motohira, Ken-ichiro Ota,* and Nobuyuki Kamiya

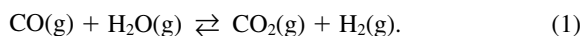
Department of Energy & Safety Engineering, Faculty of Engineering, Yokohama National University, 79-5 Tokiwadai, Hodogaya-ku, Yokohama-shi, Kanagawa 240-8501

(Received January 29, 2001)

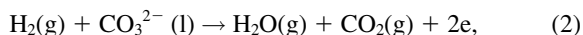
The electrochemical reduction of CO₂ to CO, which is considered to be the key reaction in a new electrochemical heat pump using the water gas shift reaction, was theoretically and experimentally investigated. Thermochemical predictions show that CO₂ can be reduced to CO below -0.8 V at 973 K. It was found that the overpotential of the electrochemical reduction of CO₂ to CO on a gold electrode was about 0.3 V at 0.01 mA cm⁻². Below -1.4 V, in the range where carbon deposition took place, CO could be produced by a chemical reaction between CO₂ and carbon. X-ray diffraction showed that the deposited carbon was not amorphous, but graphitized carbon.

A new concept for an electrochemical heat pump was proposed in order to upgrade the quality of thermal energy.^{1,2} The new electrochemical heat pump uses a combination of an electrolytic reaction at a lower temperature, absorbing low-grade thermal energy, and a thermochemical reaction at a higher temperature, producing high-grade thermal energy (Fig. 1).

The following water gas shift reaction is a possible candidate applicable to this new electrochemical heat pump:



The water gas shift reaction (1) can thermochemically proceed to the right with heat release while using an appropriate catalyst.³ When molten carbonate is used as the electrolyte, the reverse reaction of the water gas shift reaction occurs, involving the following two half-cell reactions:



In the electrolytic process, the electrical energy input enables reactions (2) and (3) to proceed to the right while absorbing heat. It has been reported that in molten carbonate the oxidation of H₂ to H₂O (reaction (2)) proceeds very easily as the anode reaction of a molten carbonate fuel cell (MCFC).^{4,5} Therefore, the reduction of CO₂ to CO (reaction (3)) is considered to be the key reaction in an electrochemical heat pump using the water gas shift reaction.

Regarding CO₂ reduction in molten carbonate, several studies have been made so far. For example, Ingram et al.⁶ experimentally investigated the formation of carbon from molten carbonate. An analysis involving X-ray powder diffraction showed that the electrodeposited carbon was amorphous. The electrochemical feature of the electrodeposited carbon was different from that of the commercial, graphitized carbon. Such differences are considered to be attributable to the porous

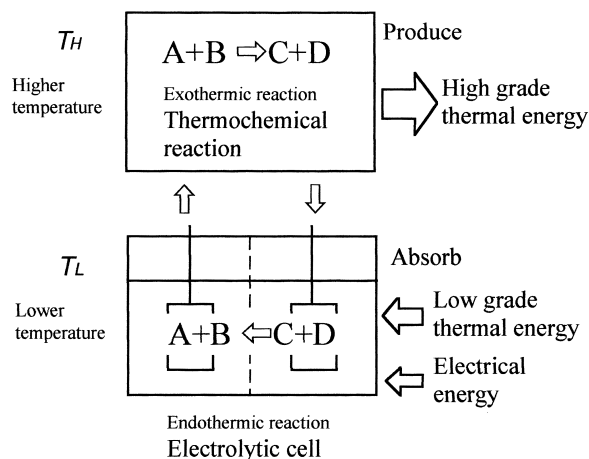


Fig. 1. Principle of a new electrochemical heat pump system.

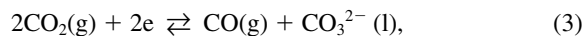
structure of the carbon. Borucka et al.^{7,8} have investigated the behavior of the CO₂/CO/Au gas electrode in the Li–Na–K ternary eutectic; they found that the equilibrium potential of this electrode accurately follows the Nernst equation over the entire range of gas compositions at temperatures of 700–800 °C. Recently, among the workers engaged in MCFC improvement, some researchers have shown interest in the reduction of CO₂ in molten carbonate. Malinowska et al.⁹ observed the reduction wave of CO₂ to CO in the Li/Na/K eutectic under 100% CO₂ at 650 °C during their study concerning the behavior of nickel species. Peelen et al.¹⁰ investigated CO₂ reduction in order to elucidate the role of CO₂ in the oxygen reduction mechanism of MCFC cathodes. They made an electrochemical study about CO₂ reduction in the 62/38 mol% Li/K eutectic under 100% CO₂ with the temperature range between 575–650 °C; they obtained the product between the square root of the diffusion constant and the solubility rate of CO₂, and concluded that CO₂ reduction to CO was reversible in that melt. However, in their paper, the chemical species were specified only

by the value of the standard electrode potential, e.g., CO was not detected by analytical instruments. Furthermore, there was no consideration of carbon deposition in their study. A complete understanding of CO₂ reduction involving carbon deposition has not yet been achieved. The purpose of this paper is to investigate the reactivity of CO₂ reduction to CO and to evaluate the effect of carbon deposition.

Thermochemical Considerations

A theoretical study was performed in order to predict the stability region of carbon species in various electrode potentials.

The following electrode reactions involving carbon species in molten carbonate have been considered:



The Nernst equations of these reactions are as follows, respectively:

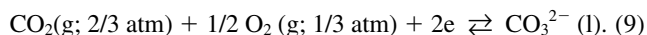
$$E(\text{CO}_2/\text{CO}) = E^0(\text{CO}_2/\text{CO}) - (RT/2F) \ln (P(\text{CO}_2)^2/P(\text{CO})), \quad (6)$$

$$E(\text{CO}_2/\text{C}) = E^0(\text{CO}_2/\text{C}) - (RT/4F) \ln P(\text{CO}_2)^3, \quad (7)$$

$$E(\text{CO}/\text{C}) = E^0(\text{CO}/\text{C}) - (RT/2F) \ln P(\text{CO})^3, \quad (8)$$

where the activity of a carbonate ion is assumed to be unity. E and P represent the electrode potential and the gas pressure, respectively. E^0 is the standard electrode potential.

The following standard oxygen electrode is used as a reference electrode:



The relationship between the equilibrium electrode potential and $P(\text{CO})$ as well as the relationship between the equilibrium electrode potential and $P(\text{CO}_2)$ can be obtained when the total pressure, $P(\text{CO}) + P(\text{CO}_2)$, is 1 atm. The Gibbs energies of the carbon species are quoted from thermochemical data.¹¹

The dependence of $P(\text{CO})$ and $P(\text{CO}_2)$ on the electrode potential at 973 K is shown in Figs. 2a and b, respectively. Fig. 2a indicates that in the range of -0.9 V – -1.048 V for reaction (3), CO₂ reduction to CO proceeds gradually to the right in accordance with the decrease in the electrode potential. In this potential range, no carbon deposition takes place, as described in Eq. 5, because the CO pressure produced through CO₂ reduction to CO (Eq. 3) is insufficient to enable the carbon deposition process shown in Eq. 5.

At -1.048 V , the electrode reactions expressed by Eqs. 3 and 5 achieve a simultaneously electrochemical equilibrium state in which the carbon, CO and CO₂ can coexist. Therefore, the Boudouard reaction (10) is in chemical equilibrium,

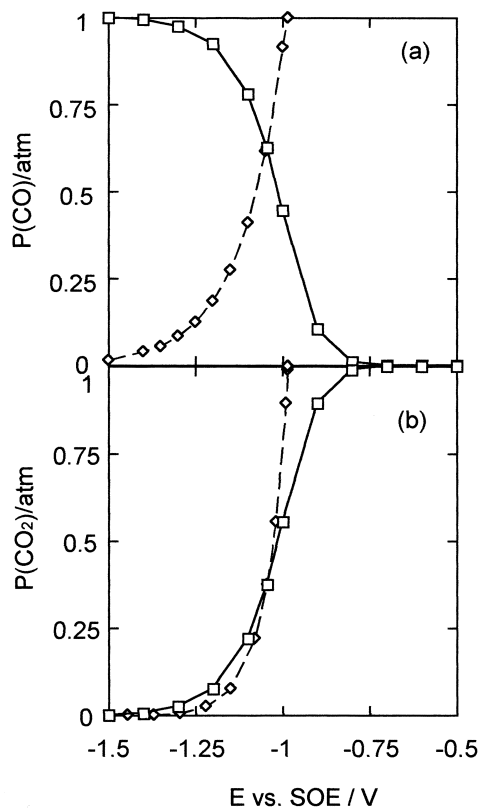
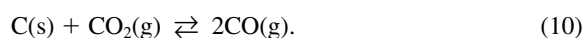


Fig. 2. Dependence of CO and CO₂ pressures on the electrode potential at 973 K.

- (a) —□— $2\text{CO}_2 + 2\text{e} = \text{CO} + \text{CO}_3^{2-}$,
 -◇- $3\text{CO} + 2\text{e} = 2\text{C} + \text{CO}_3^{2-}$.
 (b) —□— $2\text{CO}_2 + 2\text{e} = \text{CO} + \text{CO}_3^{2-}$,
 -◇- $3\text{CO}_2 + 4\text{e} = \text{C} + 2\text{CO}_3^{2-}$.

The degree of freedom of the system characterized by Eq. 10 is two. If the temperature and total pressure are fixed, the CO and CO₂ pressures are specified. Below a potential of -1.048 V , CO is unstable, because the CO pressure governed by the equilibrium between carbon and CO is always lower than the CO pressure governed by the equilibrium between CO₂ and CO. Therefore, it can be said that carbon and CO₂ are stable below a potential of -1.048 V . The equilibrium CO₂ pressure is given by Eq. 7, as shown in Fig. 2b. As described above, the maximum value of the CO pressure theoretically reaches about 0.6 atm when the total pressure is 1 atm. The maximum $P(\text{CO})$ value depends on the temperature. The dependence of the maximum $P(\text{CO})$ and $P(\text{CO}_2)$ on the temperature is depicted schematically in Fig. 3. Fig. 3 shows that at a temperature higher than 800 K, $P(\text{CO})$ increases rapidly in accordance with the temperature increase, whereas at a temperature below 750 K, only a micro amount of CO is produced by CO₂ reduction. Therefore, it leads to the conclusion that higher temperatures are more favorable for CO₂ reduction to CO. Because carbon deposition takes place only above 1200 K, almost all of the CO₂ can be reduced to CO under this condition. However, for the new electrochemical heat pump, the electrolytic reaction should proceed as an endothermic reaction at a lower temperature. Therefore, it is not practical to assume the reaction temperature to be above 1000 K. A new high-temperature electro-

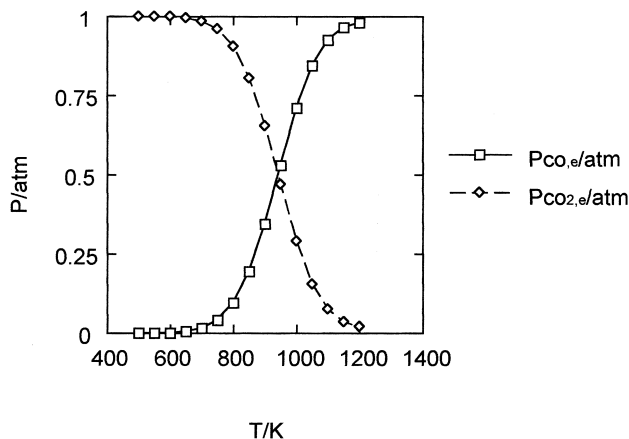


Fig. 3. Dependence of maximum CO and CO₂ pressures on temperature.

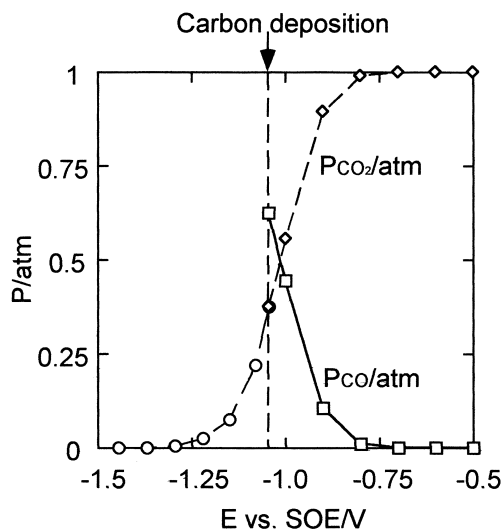
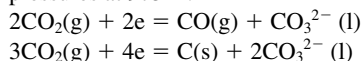


Fig. 4. Relationship between the electrode potential and gas pressures at 973 K.



chemical heat pump can be applied to the following processes, which exhaust industrial high-temperature waste heat: 1. Steel industry ((i) Coke oven 900–1050 K, (ii) Heating oven 850–1050 K); 2. Ammonia oxidation 1000–1100 K; 3. Ethylene heating 1050–1400 K and so on. According to this consideration, 973 K was selected as the reaction temperature, where the CO pressure was expected to be about 0.6 atm. The relationship between the electrode potential and the gas pressures at 973 K is shown in Fig. 4. This figure indicates that CO₂ can be reduced to CO below about -0.8 V, and that the $P(\text{CO})$ increases up to 0.6 atm in accordance with decreasing potential. It can also be seen that the disproportionation reaction of CO to CO₂ and carbon occurs below -1.048 V. Needless to say, if the carbon deposition is restrained, i.e. the overpotential of the carbon deposition is large, the CO pressure can increase even at a potential below -1.048 V.

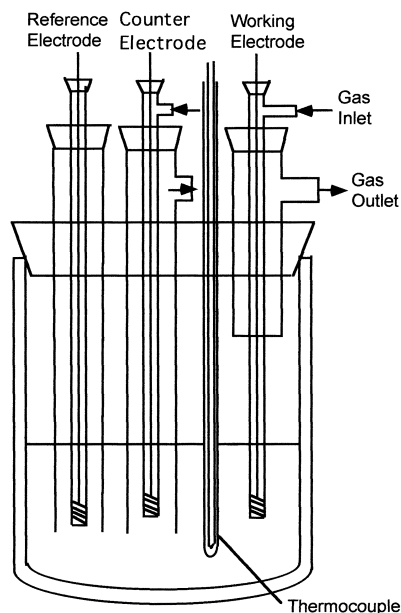


Fig. 5. Experimental cell.

Experimental

Lithium and potassium carbonates were of reagent grade from Junsei Chemicals, which were stored and mixed (in a proportion of 62 + 38 mol%) in a nitrogen-filled dry box. The amounts of the carbonates needed to produce a 150 g mixture were weighed. The salt mixture was dried at 350 °C for 12 h in a vacuum and melted at 700 °C under a CO₂ atmosphere. High-purity grade CO₂ was bubbled through the molten phase at a constant flow rate of 6 dm³ min⁻¹ under atmospheric pressure. When the potential-sweep method was performed, the bubbling was stopped. In this study, the potential sweep and the constant-potential method were carried out using a Nikko Keisoku potentiostat (NPGS-305). In the potential-sweep method, a Toho Technical Research function generator (FG-02) was used as the wave generator. The cell was a compact single-compartment cylindrical crucible (300 mm × 45 mm I.D. × 55 mm O.D.) hermetically sealed by a silicon stopper, as shown in Fig. 5. An alumina tube (5 mm I.D. × 7 mm O.D.) was used as the gas inlet. The working electrode used in the potential-sweep method was a 99.98% pure gold flag of 7 × 7 × 0.2 mm (1 cm² area) spot-welded to a gold wire ($\phi = 0.3$ mm). For the constant-potential method, large coils made of 99.98% pure gold wire ($\phi = 1$ mm) with a 20 cm length were used. Before use in the molten carbonate, the electrode surface was etched with hot concentrated hydrochloric acid, and cleaned with acetone. The reference electrode was a coiled gold wire ($\phi = 1$ mm, length = 20 cm) placed in the same atmosphere. The potential of the reference electrode was corrected by the standard oxygen electrode (SOE) in the melt. The potential of our reference electrode was 119 mV vs SOE at 973 K. This potential was in good agreement with the O₂ concentration (6.8×10^{-4} atm) in the CO₂ gas detected by gas chromatography. These results show that our reference electrode could act as a reversible oxygen electrode (ROE) in the melt. In this study, the electrode potential was expressed in vs SOE. The product gases in the constant potential method experiment were analyzed using a Shimadzu gas chromatograph (GC-8A) with the C-R5A software package. 5A molecular sieves were used as the column packing to separate O₂, N₂ and CO. The electrode surfac-

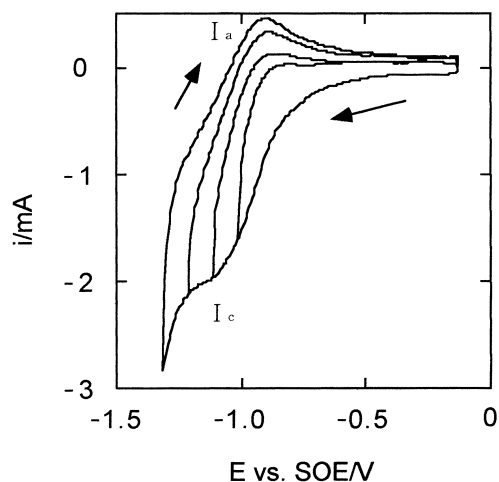


Fig. 6. Cyclic voltammograms at a gold flag electrode at lower limit of scanning potential of -1.0 , -1.1 , -1.2 and -1.3 V.

$P(\text{CO}_2) = 1$ atm; start potential -0.119 V; $v = 0.4$ V s⁻¹.

es after electrolysis were analyzed by XRD (Shimadzu XRD-6000) with a Cu target. Temperature control was achieved with an Ohkura RTC-1030 and calibrated with a chromel-alumel thermocouple.

Results and Discussion

Potential-Sweep Method. The cyclic voltammograms at several lower limits of scanning potential are shown in Fig. 6. As expressed by the figure, the reduction current started to flow below -0.8 V, the reduction wave (I_c) appeared around -1.1 V and the oxidation peak (I_a) was observed around -0.9 V. According to thermochemical predictions, the reduction wave (I_c) was attributed to the reduction of CO₂ to CO. Therefore, CO₂ reduction to CO seemed to proceed below -0.8 V. However, in this study, we could find no apparent peak of CO₂ reduction to CO around this potential, such as that observed by Peelen et al.¹⁰ Furthermore, a linear relationship between the reduction current at -1.1 V and the square root of the scanning rate could also not be obtained. It is considered that such differences were attributed to the reaction temperature. Because the reaction temperature of this study, i.e. 700 °C, was higher than that of Peelen's, i.e. 575 – 600 °C, the following possible causes were suggested: 1. Other reductions such as carbon deposition proceeded simultaneously; 2. carbonate ion as the electrolyte participated in the reduction. These assumptions should be verified by other experiments. The oxidation peak (I_a) was presumed to have a certain relation with the oxidation of CO to CO₂, because the peak (I_a) appeared only when the scanning potential was sufficiently negative below -1.1 V, the point at which CO₂ reduction to CO took place.

When the scanning potential became more negative, a large reduction current (II_c) started to flow, as shown in Fig. 7. The limiting diffusion current could not be observed, which indicated that in a lower potential region the electrolyte, carbonate ion took part in the reduction. When the lower limit of the scanning potential reached about -1.4 V, the oxidation peak (II_a) appeared. Peak (II_a) was thought to correspond to the oxidation current of deposited carbon, because the oxidation of

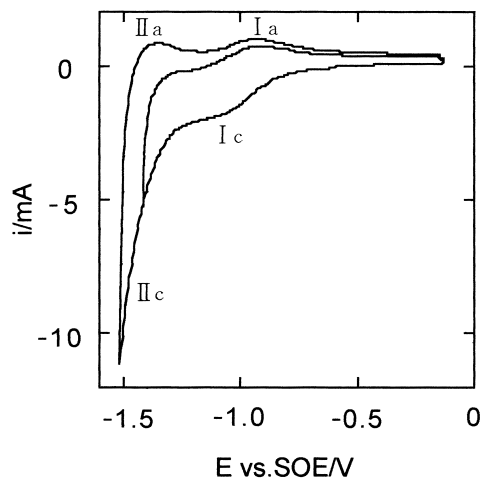


Fig. 7. Cyclic voltammograms at lower limit of scanning potential of -1.4 and -1.5 V.

$P(\text{CO}_2) = 1$ atm; start potential -0.119 V; $v = 0.4$ V s⁻¹.

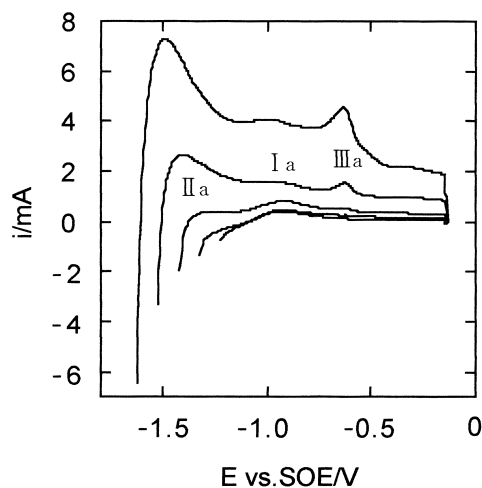


Fig. 8. Positive potential sweep voltammogram after the potential was maintained at a constant for 30 s.

CO corresponded to peak (I_a) and there was no chemical species which could be oxidized, except carbon. Therefore, it can be assumed that CO₂ and/or carbonate ion was reduced to carbon below -1.4 V.

In order to determine the exact potential at which carbon was deposited, a positive potential sweep was applied after maintaining a constant potential for 30 s. If carbon was deposited on the electrode surface, the anodic current of carbon oxidation could be observed. Figure 8 shows the results. When the maintained potential was higher than -1.3 V, anodic peak (I_a) appeared, which corresponded to CO oxidation around -0.9 V. On the other hand, when the maintained potential was lower than -1.4 V, the second anodic peak (II_a) was observed. This meant that carbon started to be deposited at -1.4 V. Under decreasing potential, peak (II_a) grew faster than peak (I_a). This implied that the rate of carbon deposition became faster than that of CO formation when the potential was maintained at less than -1.5 V. Furthermore, the third anodic peak (III_a), which could not be observed in cyclic voltammogram, ap-

peared around -0.6 V. Peak (III_a) was assumed to be caused by the oxidation of carbon, which had different electrochemical features from the carbon oxidized at peak (II_a). This, however, should be confirmed by other methods. The X-ray diffraction of deposited carbon is described later.

Constant-Potential Method. Based on thermochemical predictions and the results of the potential-sweep voltammogram, it was considered that CO₂ could be reduced to CO below -0.8 V. Therefore, the constant-potential method was performed in order to confirm CO formation below -0.8 V and to investigate the effect of deposited carbon.

Figure 9 shows the time-variations in the current density and the volume percent of CO measured at -1.3 V (no carbon deposition observed) as well as those at -1.4 V (black carbon was deposited on the surface of the electrode after electrolysis). In both cases the current rapidly reached a constant value after the double-layer capacitance was electrically charged. On the contrary, the volume percent of formed CO slowly became steady state because the cell volume was so large that it took a

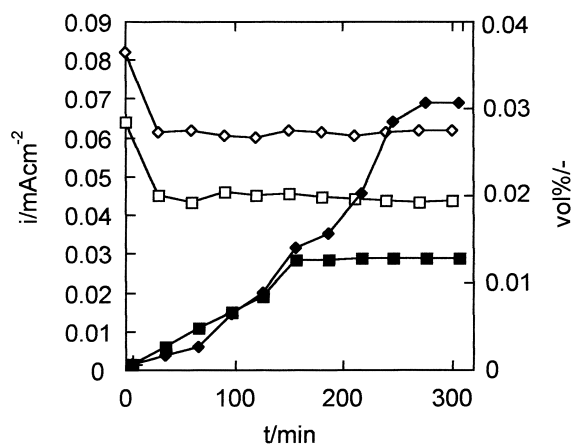


Fig. 9. Time-variations in the observed current density and the volume percent of CO formed at -1.3 and -1.4 V. Observed current density: \square -1.3 V, \diamond -1.4 V. Volume percent of formed CO: \blacksquare -1.3 V, \blacklozenge -1.4 V.

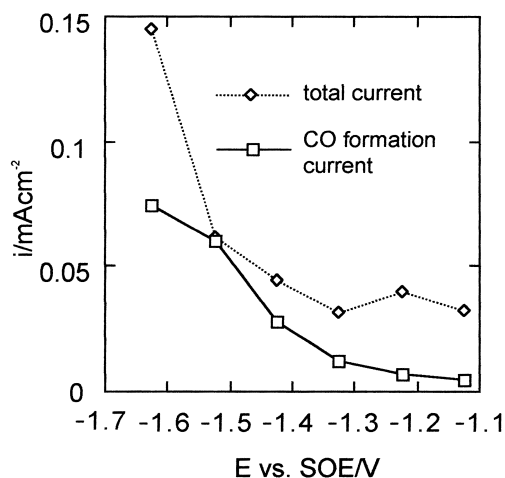


Fig. 10. Plots of the total current density and CO formation current density against the potential.

longer time for the CO to obtain a certain concentration. Figure 10 shows the whole current actually observed at each potential. It also shows the estimated CO formation current, whose value was calculated (assuming 2 electrons reaction) from the CO amount detected by gas chromatography. As shown in Fig. 10, the formed CO could be detected below -1.1 V. This was lower by ca. 0.3 V than the expected value of -0.8 V. Because the CO detection limit of the gas chromatograph was calculated to be about 10^{-4} mA cm⁻², it could be thought that above -1.1 V no CO was formed from the CO₂ reduction. Therefore, the overpotential of CO₂ reduction to CO in the constant-potential method was estimated to be ca. 0.3 V at 0.01 mA cm⁻². On the other hand, under a potential lower than -1.4 V, the carbon was observed as black color deposition on the surface of the electrode after electrolysis was completed. This result coincided with that obtained by the potential-sweep method. Thermochemically considered, the carbon should be deposited at -1.048 V. Therefore, the overpotential of carbon deposition was estimated to be about 0.35 V.

According to thermochemical considerations, in a closed system CO becomes unstable below -1.048 V due to a disproportionation reaction. Regarding the reason why CO was observed even below -1.048 V in this experiment, we considered the following: above -1.4 V, the direct process of CO₂ reduction could form CO because carbon deposition was restrained in this potential range. Below -1.4 V, deposited carbon could react with CO₂ because in an open system the CO₂ pressure at the electrode surface covered with deposited carbon was higher than the equilibrium value. Therefore, the Boudouard reaction (10) could proceed to the left. As a result, even though carbon was deposited, the rate of CO production could increase in accordance with the decreasing potential.

In the CO₂ feed gas, 6.8×10^{-4} atm of O₂ existed as an impurity. O₂ was more easily reduced than CO₂. At a higher potential in the -1.1 – -1.2 V range, O₂ reduction predominantly took place and the efficiency of the CO formation current became smaller. Below -1.4 V, a cathodic current was formed by the reduction of CO₂ into CO and carbon. After both the reduction current and the volume percent of the formed CO reached a constant value at -1.5 V, carbon deposition and CO production determined by the chemical reaction between CO₂ and carbon proceeded at the same rate. This also meant that the reduction current associated with the carbon deposition indirectly resulted in CO production. This led to the almost 100% current efficiency, measured at -1.5 V. However, in spite of the observed reduction current and the rate of CO production, which seemed to reach a steady state, the current efficiency significantly decreased below -1.6 V. This can be explained in terms of the deposited carbon; the amount of deposited carbon continuously increased because the rate of carbon deposition was higher than that of CO production from CO₂ and carbon. This resulted in a decrease in the current efficiency. In fact, below -1.6 V, a large amount of carbon deposition covered, indeed, the electrode surface after electrolysis was finished. As described above, the rate of chemical CO production from CO₂ and carbon could be regarded as a factor which governs the current efficiency as well as the electrochemical reduction of CO₂ to CO.

X-ray Diffraction. X-ray diffraction of the electrode sur-

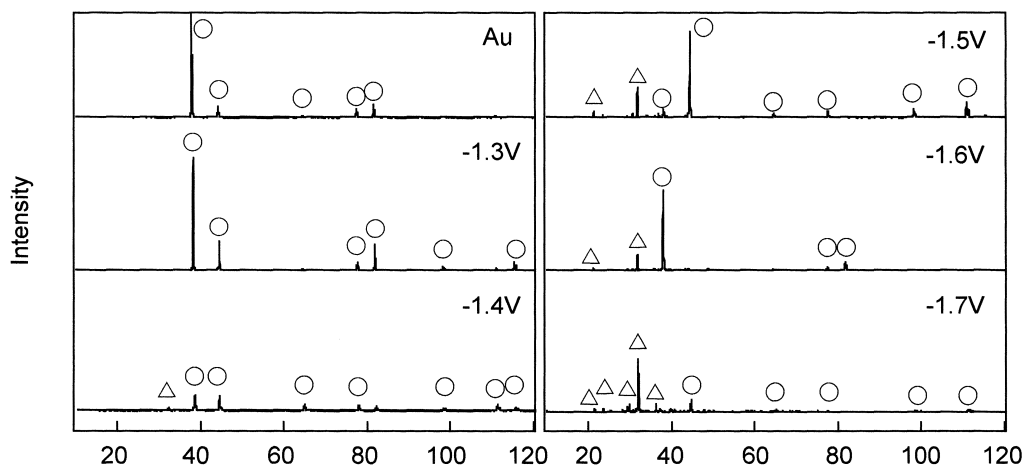


Fig. 11. X-ray diffraction pattern of the gold electrode surface after the potential was maintained at several values. ○ Au, △ Carbon.

face was performed in order to characterize the deposited carbon. Fig. 11 shows the X-ray diffraction pattern of the electrode surface after the potential was maintained at several values for a long time. As shown in Fig. 11, no peak was observed at -1.3 V, except for gold. At -1.4 V, a new peak appeared at 32 degrees. This peak corresponded to the graphitized carbon formed on the nickel at high pressures and high temperatures.¹² Ingram et al. used X-ray powder diffraction,⁶ and found out that the electrodeposited carbon was amorphous. However, in this study, a larger cathodic current could be observed even in the potential range where carbon deposition should take place. This result suggested that the deposited carbon obtained in this experiment possessed higher electrical conduction. As we assumed, the deposited carbon in this experiment was not amorphous, but graphitized carbon. It can be considered that these results were caused by a difference in the reaction temperature and/or the different composition of the investigated melt (this study; 700 °C, Li/K 62/38 mol%: Ingram et al.; 600 °C, Li/Na/K 43.5/31.5/25 mol%). On the other hand, there was no observation of carbon which related to peak (III_a). Therefore, the cause of peak (III_a) could not be clarified.

New investigations are in progress in order to obtain further experimental information on what kind of role the deposited carbon plays in the process of CO₂ reduction to CO.

Applicability of the Water Gas Shift Reaction to the New Electrochemical Heat Pump. The coefficient of performance (COP) of a heat pump is defined as the ratio of the heat output (Q_H) at a higher temperature (T_H) to the electrical energy input (W_e) at a lower temperature (T_L). As described in a previous paper,¹ the COP of a new electrochemical heat pump system was expressed as

$$\text{COP} = Q_H/W_e = T_H/(T_H - T_L) \times (1 - \eta/(\eta + U_{th})), \quad (11)$$

where U_{th} is the theoretical electrolysis voltage and η the electrolysis overvoltage. When T_H and T_L are fixed at 1023 K and 973 K, respectively, the COP dependence on η is like Fig. 12. The COP decreased rapidly with increasing η . Considering the loss of transmission of electricity and so on, COP is gener-

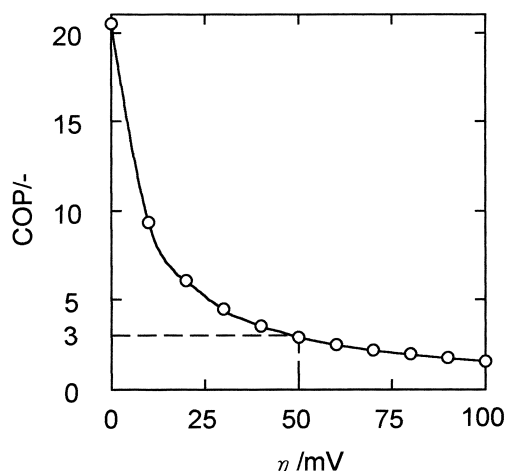


Fig. 12. Dependence of COP on η .
 $T_H = 1023$ K, $T_L = 973$ K.

ally required to be more than 3. This means that η must be lower than 50 mV under these conditions, as shown in Fig. 12. The maximum η increases in accordance with the decrease of temperature difference between T_H and T_L .

The overpotential can be decreased by means of increasing the roughness factor of the working electrode. When the roughness factor of the electrode was 100-times larger than that used in this experiment, the reduction current was also 100-times larger than that of this experiment. The standard electrode potential of the electrochemical reduction of CO₂ to CO was calculated to be -0.984 V. When a 50 mV overpotential was added, the electrode potential became ca. -1.03 V. In the case of extrapolation, the reduction current at -1.03 V was calculated to be ca. 1 mA cm⁻² according to the experimental results shown in Fig. 10. This reduction current is related to the power of an electrochemical heat pump.

Our electrochemical heat pump shows a feature in its steady state that the reduction rate at a lower temperature equals the rate of the thermochemical reaction at a higher temperature, because the reaction substances are continuously circulated between lower and higher temperature phase. The power of a

heat pump system means the rate of the thermal energy production at a higher temperature. Therefore, the product of the reduction rate at a lower temperature ($5.2 \times 10^{-5} \text{ mol sec}^{-1} \text{ m}^2$) and the enthalpy change of the water gas shift reaction at a higher temperature (-35 kJ mol^{-1}) represents the power of the electrochemical heat pump. According to the experimental results, the maximum power of the electrochemical heat pump is estimated to be about 2 W m^{-2} when the roughness factor of the electrode exceeds the experimented electrode by 100-times.

Regarding the catalysts, we should develop another material that can work more effectively for CO formation.

Conclusions

The electrochemical reduction of CO_2 to CO, which was considered to be the key reaction in the new electrochemical heat pump using the water gas shift reaction, was theoretically and experimentally investigated. Thermochemical predictions show that CO_2 can be reduced to CO below -0.8 V at 973 K and carbon can be deposited at -1.048 V . Furthermore, CO becomes unstable below -1.048 V due to a disproportionation reaction.

The electrochemical reduction was experimentally examined using a potential-sweep and constant-potential methods. The overpotential of the electrolytic reduction of CO_2 to CO on a gold electrode in the constant potential method was found to be about 0.3 V at 0.01 mA cm^{-2} , while the overpotential of carbon deposition was estimated to be about 0.35 V . Below -1.4 V in the range where carbon deposition took place, CO could be produced by the chemical reaction between CO_2 and carbon. It could be thought that the rate of chemical CO production from CO_2 and carbon governed the electrochemical reduction of the CO_2 to CO. In addition, X-ray diffraction showed that the deposited carbon was not amorphous, but graphitized carbon.

If the roughness factor of the working electrode was 100 times larger than that used in this experiment and at the same time T_H and T_L were fixed at 1023 and 973 K , respectively, the maximum power of the electrochemical heat pump could be estimated to be about 2 W m^{-2} .

This study was supported by the Original Industrial Technology R & D Promotion Program from the New Energy & Industrial Technology Development Organization (NEDO).

References

- 1 A. Ishihara, N. Motohira, K. Ota, and N. Kamiya, *J. Appl. Electrochem.*, **29**, 1079 (1999).
- 2 A. Ishihara, N. Motohira, K. Ota, and N. Kamiya, *Electrochemistry*, **67**, 450 (1999).
- 3 D. C. Ford, in "Electrochemical and Electrocatalytic Reactions of CO_2 ," ed by B. D. Sullivan, Elsevier, Oxford (1993), Chapter 3.
- 4 P. G. P. Ang and A. F. Sammells, *J. Electrochem. Soc.*, **127**, 1287 (1980).
- 5 T. Nishina, M. Takahashi, and I. Uchida, *J. Electrochem. Soc.*, **137**, 1112 (1990).
- 6 M. D. Ingram, B. Baron, and G. J. Janz, *Electrochim. Acta*, **11**, 1629 (1966).
- 7 A. Borucka, *Electrochim. Acta*, **13**, 295 (1968).
- 8 A. Borucka and C. M. Sugiyama, *Electrochim. Acta*, **14**, 871 (1969).
- 9 B. Malinowska, M. Cassir, F. Delcorso, and J. Derynck, *J. Electroanal. Chem.*, **389**, 21 (1995).
- 10 W. H. A. Peelen, K. Hemmes, and J. H. W. de wit, *Electrochim. Acta*, **43**, 763 (1997).
- 11 I. Barin, "Thermochemical Data of Pure Substances," 3rd ed, VCH, Weinheim (1995), Vol. 1.
- 12 L. E. Shterrenberg and S. V. Bogdanova, *Inorg. Mater.*, **1979**, 632.